Published in final edited form as:
Biochemistry. 2011 December 6; 50(48): 10508–10519. doi:10.1021/bi201430f.

Biosynthesis and antimicrobial evaluation of backbone-cyclized alpha-defensins[#]

Angie E. Garcia[1], **Kenneth P. Tai**[2], **Shadakshara S. Puttamadappa**[3], **Alexander Shekhtman**[3], **Andre J. Ouellette**[2], and **Julio A. Camarero**[1,*]

[1]Department of Pharmacology and Pharmaceutical Sciences and University of Southern California, Los Angeles, CA 90033, USA

[2]Department of Pathology and Laboratory Medicine, University of Southern California, Los Angeles, CA 90033, USA

[3]Department of Chemistry, State University of New York, Albany, NY 12222, USA

Abstract

Defensins are antimicrobial peptides that are important in the innate immune defense of mammals. Upon stimulation by bacterial antigens, enteric α-defensins are secreted into the intestinal lumen where they have potent microbicidal activities. Cryptdin-4 (Crp4) is an α-defensin expressed in Paneth cells of the mouse small intestine and the most bactericidal of the known cryptdin isoforms. The structure of Crp4 consists of a triple-stranded antiparallel β-sheet, but lacks three amino acids between the fourth and fifth cysteine residues, making them distinct from other α-defensins. The structure also reveals that the α-amino and C-terminal carboxylic groups are in proximity (d ≈ 3 Å) in the folded structure. We present here the biosynthesis of backbone-cyclized Crp4 using a modified protein splicing unit or intein. Our data show that cyclized Crp4 can be biosynthesized by using this approach both *in vitro* and *in vivo*, although the expression yield was significantly lower when produced inside the cell. The resulting cyclic defensins retained the native α-defensin fold and showed equivalent or better microbicidal activities against several Gram-positive and Gram-negative bacteria when compared to native Crp4. No detectable hemolytic activity against human red blood cells was observed for either the native or cyclized variants of Crp4. Moreover, both forms of Crp4 also showed high stability to degradation when incubated with human serum. Altogether, these results indicate the potential for backbone cyclized defensins in the development of novel peptide-based antimicrobial compounds.

The cyclization of peptides has commonly been used to generate more active and stable scaffolds for therapeutic purposes (1–6). In general, backbone-cyclized peptides are more resistant than linear peptides to chemical, thermal, and enzymatic degradation (7). Since circular peptides have no N- and C-terminus, they are more rigid, endowing them with the ability to persist in physiologic environments such as blood serum (3, 6).

The production of backbone cyclized or circular peptides can be performed chemically by using solid-phase peptide synthesis in combination with native chemical ligation (8–13) or recombinantly in bacteria by using modified protein splicing units or inteins (14–16). The latter method has been used for the biosynthesis of several disulfide-rich cyclic peptides

[*]Corresponding author: Julio A. Camarero, Ph.D. Associate Professor Department of Pharmacology and Pharmaceutical Sciences School of Pharmacy University of Southern California 1985 Zonal Avenue, PSC 616 Los Angeles, CA 90033 Phone: 323-442-1417; camarej@usc.edu.

Supporting Information It contains supplementary results mentioned in the text, including two tables and seven figures. This material is available free of charge via the Internet at http://pubs.acs.org.

such as cyclotides (17, 18) and sunflower trypsin inhibitor 1 (SFTI-1) (19). The expression of cyclic peptides *in vivo* has many applications including the generation of peptide libraries for high-throughput screening of biological activities such as antimicrobial activity or specific inhibition of protein-protein interactions involved in various pathologies.

Mammalian defensins are a family of disulfide-stabilized, host defense peptides (20–24). They are classically known for their antimicrobial activities, but have many other defense mechanisms including wound healing (25, 26), immune modulation (27–30), neutralization of endotoxin (31–33), and anti-cancer activities (34). Mammalian defensins are cationic peptides with largely β-sheet structures and six conserved cysteines, which form three intramolecular disulfide bonds (Fig. 1). They are divided into three structurally distinct groups, α-, β-, and θ-defensins. The overall fold of α- and β-defensins is quite similar despite differences in disulfide connectivities, and the presence of an N-terminal α-helix segment in β-defensins that is lacking in α-defensins (35). θ-Defensins, on the other hand, are cyclic peptides formed by the head-to-tail covalent assembly of two nonapeptides, and to date, are the only known cyclic polypeptides expressed in animals (22).

The antibacterial activity of α- and β-defensins is highly dependent on the ionic strength of the media, and salt-dependent inactivation of defensins in patients with cystic fibrosis has been proposed as the potential cause of chronic pulmonary infections in these patients (36). The antimicrobial activity of the naturally cyclic θ-defensins, in contrast, has been shown to be less sensitive to salt concentration than α- and β-defensins (22). This difference has been attributed to the circular structure of θ-defensins since the acyclic forms are more salt sensitive (22). In agreement with this, replacement of Cys pairs to Gly in the rabbit α-defensin neutrophil peptide 1 (NP-1) and backbone cyclization provided biologically active defensin analogs that were less sensitive to salt (37). However no studies were performed on the stability of these analogs.

Intrigued by these results we decided to investigate further the effects of backbone cyclization on the activity and stability of fully folded α-defensins. In this work, we have used the α-defensin cryptdin-4 (Crp4) from murine Paneth cells as a model system (38). Cryptdins are secreted into the crypt lumen by mouse small intestinal Paneth cells (39–42) where they exert potent microbicidal effects and determine the composition of the ileal microbiome (38, 43–45). Cryptdins show very similar antibacterial activity against Gram-positive and Gram-negative bacteria, with Crp4 displaying the greatest microbicidal activity in *in vitro* assays (46). Cryptdins are classified as enteric defensins and homologs have been found in other mammals (42, 47). The structure of Crp4 consists of a triple-stranded antiparallel β-sheet (35), but lacks three amino acids between the fourth and fifth cysteine residues, making them distinct from other α-defensins (Fig. 1). The structure also reveals that the α-amino and C-terminal carboxylic groups are proximal in the folded structure (Fig. 1) suggesting that the introduction of backbone cyclization at this point could help to stabilize the defensin scaffold without disrupting its structure and biological activity.

Here we present the recombinant expression and characterization of several backbone cyclized analogs of fully folded Crp4. Backbone cyclization was performed *in vitro* and *in vivo* using an intramolecular intein-mediated cyclization in *Escherichia coli* cells (48). The expression yields of folded cyclized Crp4 *in vivo* were, however, lower than those obtained when the cyclization and folding was performed *in vitro* from the intein fusion precursors. Our data also show that cyclized versions of Crp4 adopt a native folded structure and show equal or better microbicidal activities against several Gram-positive and Gram-negative bacteria than native Crp4 (Crp4-wt). Native and cyclized variants of Crp4 were antimicrobial in the presence of human serum, and the biological activity of cyclized Crp4 was slightly less affected by the presence of 160 mM sodium chloride than native Crp4.

Also, neither native or cyclized Crp4 showed detectable hemolytic activity against human red blood cells. Moreover, both native and cyclized Crp4 showed remarkable resistance to degradation in 100% human serum with half-life values greater than 48 h. Altogether, these results indicate that backbone cyclization provides a means for engineering defensins to improve biological activity while providing excellent stability to serum degradation, highlighting the potential of these peptide scaffolds for the development of novel antimicrobial compounds.

EXPERIMENTAL PROCEDURES

Analytical reverse phase (RP)-HPLC was performed on a HP1100 series instrument with 220 nm and 280 nm detection using a Vydac C4 or C18 column (5 mm, 4.6 × 150 mm) at a flow rate of 1 mL/min. Semipreparative RP-HPLC was performed on a Waters Delta Prep system fitted with a Waters 2487 Ultraviolet-Visible (UV-vis) detector using a Vydac C4 column (5 μm, 10 × 250 mm) at a flow rate of 5 mL/min. All runs used linear gradients of 0.1% aqueous trifluoroacetic acid (TFA, solvent A) vs. 0.1% TFA, 90% MeCN in H_2O (solvent B). UV-vis spectroscopy was carried out on an Agilent 8453 diode array spectrophotometer. Electro-spray mass spectrometry (ES-MS) was performed on an Applied Biosystems API 3000 triple quadrupole mass spectrometer. Calculated masses were obtained by using ProMac v1.5.3. Protein samples were analyzed by SDS-PAGE 4–20% Tris-Glycine Gels (Lonza, Rockland, ME). The gels were then stained with Pierce (Rockford, IL) Gelcode Blue, photographed/digitized using a Kodak (Rochester, NY) EDAS 290, and quantified using NIH Image-J software (http://rsb.info.nih.gov/ij/). DNA sequencing was performed by the DNA Sequencing and Genetic Analysis Core Facility at the University of Southern California using an ABI 3730 DNA sequencer, and the sequence data was analyzed with DNAStar (Madison, WI) Lasergene v8.0.2. All chemicals were obtained from Sigma-Aldrich (Milwaukee, WI) unless otherwise indicated.

Cloning and in vitro expression of backbone cyclized Crp4 variants

Synthetic DNA oligos (Integrated DNA technologies, Coralville, IA) encoding the different backbone cyclized Crp4 analogs (Table S1) were annealed and ligated into the pTXB1 vector (New England Biolabs, Ipswich, MA) using the NdeI and SapI restriction sites as described previously.(17, 49) The resulting plasmids were transformed into either BL21(DE3) or Origami2(DE3) cells (EMD Chemicals, Gibbstown, NJ) and grown in LB broth. Transformed BL21(DE3) cells were induced with 0.3 mM IPTG for 4 h at 30 °C and transformed Origami2(DE3) cells with 0.1 mM IPTG for 20 h at 22 °C. Cells were lysed in 0.1 mM EDTA, 1 mM PMSF, 50 mM sodium phosphate, 250 mM sodium chloride buffer at pH 7.2 containing 5% glycerol by sonication. The soluble fraction was incubated with chitin beads (New England Biolabs) for 1 h at 4°C and the beads were washed with column buffer (0.1 mM EDTA, 50 mM sodium phosphate, 250 mM sodium chloride buffer at pH 7.2) containing 0.1% Triton X-100 followed by washes with column buffer without Triton X-100. The peptide was cyclized and folded *in vitro* using column buffer at pH 7.2 containing 50–100 mM reduced glutathione (GSH) for 2–3 days at room temperature with gentle rocking. We found that under these conditions backbone cyclized Crp4 variants bind strongly to the chitin column, and therefore were eluted using 8 M GdmCl in water. The corresponding supernatant and washes were pooled, and the backbone cyclized Crp4 peptides were purified by semipreparative HPLC using a linear gradient of 20–40% solvent B over 30 min. Purified products were characterized by HPLC and ES-MS. All Crp4 variants were quantified by UV-VIS using a molar absorption coefficient value of 3365 M^{-1} cm^{-1}. The expression of Crp4-intein fusion precursors were quantified by first desorption of the proteins from an aliquot of chitin beads using 8 M GdmCl and then measurement by UV-VIS using a molar absorption coefficient value of 39,015 M^{-1} cm^{-1}.

Preparation of Crp4-R/A

The linear reduced and alkylated Crp4 (Crp4-R/A) was produced by expression of the Crp4-1 intein precursor in BL21(DE3) cells using the induction conditions described above. After purification of the fusion with chitin beads, Crp4-1 was cleaved from the intein using 100 mM NH_2-OH in water at pH 7.2 for 18 h at room temperature. The resulting linear Crp4-1 peptide was reduced with 5 mM DTT at 37 °C for 3 h and alkylated with 12.5 mM iodoacetamide for 10 min at room temperature. Crp4-R/A was purified by semipreparative HPLC as described above. The purified product was characterized by HPLC and ES-MS (Fig. S7).

Expression of native Crp4-wt and Crp4-6C/A

Native Crp4-wt and Crp4-6C/A were expressed in *E. coli*, purified and refolded as previously described (50, 51).

Expression of ^{15}N-labeled backbone cyclized Crp4 variants

Expression was carried out using BL21(DE3) cells as described above except grown in M9 minimal medium containing 0.1% $^{15}NH_4Cl$ as the nitrogen source (18, 52). Cyclization and folding was performed as described above. The ^{15}N-labeled backbone cyclized Crp4 defensins were purified by semipreparative HPLC as before. Purified products were characterized by HPLC and ES-MS (Fig. S3).

In vivo expression of Crp4-1

Origami2(DE3) cells transformed with the plasmid encoding the intein precursor of Crp4-1 were induced, harvested and lysed as described above. The insoluble pellet was first washed three times with column buffer containing 0.1% Triton X-100 and then twice with just column buffer. The resulting pellet was dissolved in minimal amount of 8 M GdmCl in water. Both the soluble cell lysate and solubilized cell lysate pellet were extracted using C18 SepPak cartridges (Waters, Milford, MA) with elution in MeCN:H_2O (3:2 vol.) containing 0.1% TFA. The samples were analyzed by HPLC-tandem mass spectrometry (MS/MS) using a C18-HPLC column (5 mm, 2.1 × 100 mm), and H_2O-MeCN buffers containing 0.1% formic acid as mobile phase. Typical analysis used a linear gradient of 0%–90% MeCN in H_2O over 10 min. Detection was performed on an API 3000 ES-MS using a multiple reaction-monitoring (MRM) mode. Data were collected and processed using Analyst software (Applied Biosystems). The calibration curve using purified cyclic Crp4-1 was found to be linear in the range of 5–50 ng.

NMR spectroscopy

NMR samples were prepared by dissolving ^{15}N-labeled backbone cyclized Crp4 variants into 80 mM potassium phosphate in 90% H_2O/10% ^2H_2O (v/v) or 100% D_2O to a concentration of approximately 0.2 mM with the pH adjusted to 4.5 or 6.0 by addition of dilute HCl. All ^{1}H NMR data were recorded on a Bruker Avance II 700 MHz spectrometer equipped with a cryoprobe. Data were acquired at 27 °C, and 2,2-dimethyl-2-silapentane-5-sulfonate, DSS, was used as an internal reference. All 3D experiments, $^1H\{^{15}N\}$-TOCSY-HSQC and $^1H\{^{15}N\}$-NOESY, were performed according to standard procedures(53) with spectral widths of 12 ppm in proton dimensions and 35 ppm in nitrogen dimension. The carrier frequency was centered on the water signal, and the solvent was suppressed by using WATERGATE pulse sequence. TOCSY (spin lock time 80 ms) and NOESY (mixing time 150 ms) spectra were collected using 1024 t_3 points, 256 t_2 anf 128 t_1 blocks of 16 transients. Spectra were processed using Topspin 1.3 (Bruker). Each 3D-data set was apodized by 90°-shifted sinebell-squared in all dimensions, and zero filled to 1024 × 512 ×

256 points prior to Fourier transformation. Assigments for the backbone nitrogens, H^{α} and H' protons (Figs. S4, Tables S2 and S3) were obtained using standard procedures (53, 54).

Bactericidal peptide assays

Native Crp4 (Crp4-wt) and backbone cyclized Crp4 variants were tested for bactericidal peptide activity against Gram-negative and Gram-positive bacteria. Bacteria growing exponentially in trypticase soy broth (TSB) were centrifuged at 10,000 × g for 3 min and washed three times with 10 mM PIPES buffer at pH 7.4 supplemented with 1% (vol/vol) of TSB (10 mM PIPES-TSB). Approximately 1–5 × 10^6 colony forming units (CFU)/ml of bacteria were incubated with peptides in a total volume of 50 μL of 10 mM PIPES-TSB. In assays performed in the presence of salt or serum, sample mixtures were incubated in 10 mM PIPES-TSB supplemented with sodium chloride or heat-inactivated human serum, respectively. Bacterial-peptide mixtures were incubated at 37 °C with shaking for 1 h, 20 μL aliquot samples were diluted in 2 mL 10 mM PIPES buffer at pH 7.4, and plated on TSB plates using an Autoplate 4000 (Spiral Biotech Inc., Bethesda, MD). After incubation overnight at 37°C, bacterial cell survival was determined by counting CFUs.

Hemolysis assay

EDTA-anti-coagulated human blood was obtained from a healthy donor (Bioreclamation, LLC, Hicksville, NY) and centrifuged at 234 × g for 10 min at 22 °C. Red blood cells (RBCs) were washed four times with Dulbecco's phosphate-buffered saline (DPBS, Mediatech Inc, Manassas, VA) containing 4 mM EDTA and resuspended in DPBS without EDTA. Peptides diluted in DPBS to the concentrations shown were assayed for hemolysis in triplicate by incubation with 2% RBCs (vol/vol) for 1 h at 37 °C in an atmosphere of 5% CO_2. The cells were centrifuged at 234 × g for 10 min at 22°C and the absorbencies of the supernatants were measured at 405 nm. Hemolytic activity of each peptide was calculated relative to the 100% hemolysis obtained by incubation of RBCs with 1% Triton X-100.

Serum stability assay

Peptides at 100 μg/mL (~27 μM) in human serum (Lonza) were incubated at 37 °C. After various time points, triplicate serum aliquots were removed, quenched with 6 M urea in water, and incubated for 10 min at 4 °C. Subsequently, serum proteins were precipitated with 20% trichloroacetic acid for 10 min at 4 °C and centrifuged at 13,000 rpm for 10 min at 4 °C. The supernatants were analyzed by C4 RP-HPLC and the pellets were dissolved in 8 M GdmCl and also analyzed by HPLC. The percentage of peptide recovery was determined by integration of the HPLC peaks at 220 nm. Peptide identity was also confirmed by ES-MS.

RESULTS

Design of backbone cyclized Crp4 defensins

The biosynthesis of backbone cyclized Cys-rich polypeptides using modified protein-splicing units or inteins has previously been demonstrated for several cyclotides (17, 18, 49, 52) and sunflower trypsin inhibitor 1 (SFTI-1) (55). Here, we have used a similar strategy for the biosynthesis of several backbone cyclized Crp4 variants in *E. coli* cells. This approach makes use of a modified intein in combination with an intramolecular native chemical ligation reaction (NCL) (Fig. 2) (17, 49). Intramolecular NCL requires the presence of an N-terminal Cys residue and a C-terminal α-thioester group in the same linear precursor molecule (8, 14). For this purpose the corresponding Crp4 linear precursor was fused in frame at the N- and C-terminus to a Met residue and a modified *Mxe* Gyrase A intein, respectively. This allows the generation of the required C-terminal thioester and N-

terminal Cys residue after *in vivo* processing by endogenous Met aminopeptidase (MAP) (Fig. 2). We designed five linear Crp4 precursors (Crp4-1 to -5) to explore the best ligation site as well as the best linker required for optimal cyclization and folding of the resulting backbone cyclized Crp4 variants (Scheme 1 and Table 1). We first decided to link together through a peptide bond the native N- and C-terminal residues in Crp4-wt, Gly1 and Arg32 respectively. These two residues are in proximity in the folded structure of Crp4-wt and in principle the formation of this bond should not introduce too much conformational stress in the new loop formed. To facilitate the ligation we used Cys^{I} (Crp4-1), Cys^{II} (Crp4-4) and Cys^{V} (Crp4–5) as the N-terminal residue in the corresponding linear precursors (Table 1). In addition, we also explored the effect of adding extra residues in the new loop formed in the backbone cyclized Crp4. Hence, we added an extra Gly residue (Crp4-2) and a Pro-Gly sequence (Crp4-3) between the native N- and C-terminal residues, Gly1 and Arg32 respectively (Table 1). These two additions should increase the flexibility of the new loop as well as facilitate the formation of the required turn (56). In these two variants we only used Cys^{I} as the N-terminal residue to allow for the cyclization reaction.

In vitro biosynthesis of backbone cyclized Crp4 peptides

All five linear Crp4-intein fusion precursors were expressed in BL21(DE3) cells at 30 °C and purified by affinity chromatography using chitin-sepharose beads. The Crp4-intein precursors have a chitin binding domain (CBD) fused at the C-terminus of the intein domain to facilitate purification. The expression yields of the different Crp4-intein constructs in the soluble cell lysate were estimated by UV spectroscopy and ranged from ≈ 5 mg/L for intein precursor Crp4–1 to ≈14 mg/L for precursor Crp4–5 (Table 2). The rest of the constructs gave similar expression yields in the soluble fraction (≈ 10 mg/L). All of the linear precursors using Cys^{I} as the N-terminal residue (Crp4–1, Crp4–2 and Crp4–3) also produced a significant amount of protein in the insoluble fraction ranging from 142 mg/L for Crp4–1 (≈90% of the total precursor expressed) to 24 mg/L for Crp4–2 (≈70% of the total precursor expressed). Interestingly, neither precursor Crp4-4 or Crp4–5 showed any significant expression in the insoluble fraction (Fig. S1), suggesting that the arrangement of the Crp4 peptide primary sequence plays an important role in the folding of the precursors and subsequent shuttling to inclusion bodies. Analysis of the purified fusion proteins by SDS-PAGE (Fig. S1) revealed that all of the linear precursors except Crp4–5 showed ≈ 20% cleavage of the intein fusion *in vivo* when expressed in BL21(DE3) cells for 4 h at 30 °C. In contrast, precursor Crp4–5 gave only 7% *in vivo* cleavage.

We next tested the ability of the different precursors to be cleaved *in vitro* using reduced glutathione (GSH). GSH has been shown to promote cyclization and concomitant folding when used in the biosynthesis of Cys-rich cyclic polypeptides (18, 49, 55). The cyclization/folding reaction was performed on the chitin beads where the corresponding precursors had been purified. The best cleavage/cyclization conditions were accomplished using 100 mM of GSH in phosphate buffer at pH 7.2 for 48 h. Under these conditions ≈85% of the precursor for Crp4–1 was cleaved *in vitro* (Table 2 and Fig. S1). Precursors Crp4–2 and Crp4–3 were also cleaved efficiently (≈70%) under these conditions. In contrast, linear precursors Crp4-4 and Crp4–5 were cleaved less efficiently by GSH, ≈65% for Crp4-4 and ≈45% for Crp4–5. HPLC analysis of the crude cyclization mixture revealed in all the cases the main peptide product was the corresponding folded backbone cyclized Crp4 variant as revealed by ES-MS analysis (Figs. 3 and S2). Other peptide peaks in the HPLC chromatograms were identified as not correctly folded GSH-adducts. Among the different linear precursors, Crp4–1 gave the best cyclization/folding yield (Fig. 3A) producing around 200 μg/L of cyclized Crp4–1 (≈50% of theoretical yield, see Table 1). The cyclization/folding crude mixture for Crp4–2 and Crp4–3 (Figs. 3B and 3C), both using the same ligation site as Crp4–1 but with different linker lengths for the new loop formed at the ligation site, gave

lower yields (≈120 and 170 μg/L, respectively) than Crp4–1. The HPLC trace for the cyclization reaction of precursor Crp4–3 was, however, cleaner than that of Crp4–2 indicating the cyclization/folding was more efficient in that precursor (Figs. 3B and 3C). The cyclization/folding yields for Crp4-4 and Crp4–5 (Fig. S2) were similar and estimated by HPLC to be around 40 μg/L and 35 μg/L, respectively (Table 2). These lower yields could be attributed, in part, to the less efficient cleavage of the intein in these precursors.

It is worth noting that during the cleavage of the intein precursors we found that the corresponding cyclized Crp4 peptides were able to bind strongly to the chitin beads under the conditions used for the GSH-induced cyclization/folding, and required the use of 8 M GdmCl to elute the cyclized peptides from the solid support. This treatment also eluted the intein-CBD protein by-product (Fig. 3). Accordingly, we tested whether the cyclized Crp4 variants were binding to the chitin-sepharose beads or intein-CBD protein by incubating purified cyclized Crp4–1 with either free, CBD bound, or intein-CBD bound chitin-sepharose beads. After extensive washing, the beads in both cases were washed with 8 M GdmCl and the amount of eluted Crp4–1 quantified by HPLC. The results showed that approximately ≈25% was able to bind free or CBD bound chitin beads, and ≈90% of cyclized Crp4–1 was bound to intein-CBD chitin beads (data not shown). This demonstrates that although cyclized Crp4 has some small affinity for chitin-sepharose beads, it was bound to the beads mainly by protein-protein interactions with the Gyrase intein.

Structural characterization of cyclized Crp4 defensins

Since the structure of native Crp4-wt has been elucidated by ^{1}H-NMR (35), we used heteronuclear NMR spectroscopy to confirm that the biosynthetic cyclized Crp4 defensins were adopting a native α-defensin fold. Given that Crp4-wt and cyclized Crp4–1 have the same sequence, we first compared the assigned backbone amide and alpha (H' and H^{α}) proton chemical shifts of cyclized Crp4–1 with those published for the native Crp4-wt peptide (Table S2) (35). As shown in Figure 4, the chemical shift differences for most of the residues were smaller than 0.1 ppm, which indicates that cyclized Crp4–1 adopts a structure that is very similar to that of native Crp4-wt. We also saw a few residues that showed chemical shift differences higher than 0.1 ppm. Most of these residues, however, were located in the new loop formed close to the cyclization site, and include residues Leu2, Leu3, Cys4 and Cys29 (Fig. 4A). Interestingly, we also noticed a few residues (His10, Arg16 and Arg18) located away from the ligation site that presented relatively large chemical shift differences (Fig. 4A). The chemical shift difference associated with the H' of Arg16 was ≈0.4 pm, meanwhile for the other residues the corresponding differences were relatively smaller (≈0.1 ppm). Based on these changes, it is very likely that the hydrogen bond between the carbonyl group of Cys29 and the H' of Arg16 present in the structure of native Crp4-wt is broken in cyclized Crp4–1. This change would lead to changes in the backbone dihedral angles of the neighboring amino acids. This is in agreement with the fact that the differences observed for the chemical shits of the side chain protons, H^{β}, are all smaller than 0.1 ppm (Fig. 4D and Table S2).

We also used heteronuclear $^{1}H\{^{15}N\}$-HSQC experiments to compare the structures of the different cyclized Crp4 variants. Uniformly ^{15}N-labeled cyclized Crp4 defensins were produced *in vitro* as described above but *E. coli* was grown in minimal M9 medium containing $^{15}NH_4Cl$ as the only source of nitrogen. Recombinant expression of cyclized Crp4 defensins allows the introduction of NMR active isotopes (^{15}N and/or ^{13}C) in a very inexpensive fashion, thus facilitating the use of the SAR by NMR (structure-activity relationship by nuclear magnetic resonance) (57, 58) technique to study any molecular interaction between cyclized Crp4 defensins and their potential biomolecular targets. The HSQC spectra for all of the cyclized Crp4 variants were very well dispersed, indicating a well folded structure (Fig. S5). As expected, the chemical shift differences for the backbone

amide between the different cyclized Crp4 variants were also relatively small with the major differences located in residues close to the ligation site and to Arg16 (Fig. S5). As expected, analysis of the HQSC spectrum of Crp4–2 revealed the presence of an additional Gly peak as compared to the spectrum of Crp4–1 (Fig. S5B). In contrast, analysis of the HSQC spectrum of Crp4–3 revealed as many as 9 additional peaks (Fig. S5B). Careful integration of the intensities associated with the HSQC spectrum of cyclized Crp4–3 showed that 18 crosspeaks have intensities approximately two times lower than the rest of the peaks. These findings suggest that 9 residues in cyclized Crp4–3 have two different conformations that could be exchanging at a very low rate or not at all. We attributed the existence of two Crp4–3 conformations in solution to *cis-trans* isomerization of the proline in the new loop formed since most of the residues exhibiting amide peaks doubling were located close to the newly formed loop.

In vivo biosynthesis of cyclized Crp4 defensins

Encouraged by the results obtained with the *in vitro* GSH-induced cyclization/folding of the intein-Crp4 precursors we decided to explore the expression of cyclized Crp4 inside *E. coli* cells. To accomplish this, we used the intein precursor Crp4–1. This construct gave the best yield for the production of cyclized Crp4–1 *in vitro* (Table 2). The production of cyclized Crp4–1 was accomplished in Origami2(DE3) cells. These cells have mutations in the thioredoxin and glutathione reductase genes, which facilitates the formation of disulfide bonds in the bacterial cytosol (59). We have recently used these cells for the *in vivo* production of several disulfide-containing backbone cyclized polypeptides (17, 18, 55).

The expression yield for the Crp4–1 precursor after overnight induction at room temperature with IPTG was approximately 5.5 mg/L. Under these conditions around 35% of the Crp4-intein precursor was cleaved *in vivo* (Fig. 5A). Using these numbers we estimated the maximum amount of cyclized Crp4–1 peptide that could be produced should be around 200 μg/L. Initial attempts to identify and quantify the amount of cyclized Crp4–1 *in vivo* by HPLC found there to be very low amounts associated with the insoluble cell lysate and none detected in the soluble fraction. We were able to quantify the amount of cyclized Crp4–1 present in the insoluble cellular fraction using HPLC-MS/MS (Fig. 5B). The yield was estimated to be ≈2 μg/L, 100-fold lower than expected (≈1% yield). The cyclized Crp4–1 obtained *in vivo* had the mass corresponding to the folded product and co-eluted with the purified product obtained *in vitro*, indicating that they were the same compound. The low efficiency observed for the expression *in vivo* could be attributed to the toxicity of this defensin. α-Defensins are antimicrobial compounds that can bind and disturb the membranes of bacteria and have also been shown to inhibit the biosynthesis of peptidoglycan by binding to its precursor lipid II (60, 61). It is likely that folded cyclized Crp4 may exert the same type of action when it is in the bacterial cytosol and could explain why Crp4–1 was found in the insoluble cell lysate. Moreover, we have shown that cyclized Crp4 defensins have affinity for the intein-CBD protein fusion and therefore any precursor protein present in the insoluble pellet could also bind cyclized Crp4 defensins facilitating its immobilization to the insoluble cell lysate.

We also examined the expression of cyclized Crp4 defensins using the Crp4–4 and Crp4–5 precursors (Fig. S1), especially since the Crp4–5 precursor gave better *in vivo* cleavage (≈70%). Based on the expression levels, the predicted yield for Crp4–4 is approximately 20 μg/L and for Crp4–5, almost 200 μg/L. In both cases, the corresponding folded cyclized Crp4 variant was found in the insoluble cell lysate with similar yields to the one found for Crp4–1 (1–2 μg/L). These three precursors gave very different yields for cyclization/folding when performed *in vitro*. The fact that they provide a similar yield when expressed *in vivo* may suggest that the production *in vivo* could be limited by the cellular activity of the defensin.

Antimicrobial and hemolytic activities of cyclized Crp4 defensins

Native Crp4-wt has potent antimicrobial activities against a broad spectrum of microorganisms, including Gram-positive and Gram-negative bacteria (42, 46, 62). In order to explore the effect of cyclization on its biological activity, we tested the antimicrobial activities of the cyclized Crp4 defensins against several Gram-positive and Gram-negative bacteria. As shown in Figure 6, all cyclized defensins showed a dose-dependent killing of the bacteria tested, including methicillin-resistant *Staphyloccocus aureus* (MRSA) strain EB378 and enteropathogenic *E. coli* (EPEC) strain E2348/69. Overall, the cyclic peptides were most active against *Listeria monocytogenes* 10403s, killing 90–100% at 10 μg/mL, and were least active against *Salmonella typhimurium* 14028s, but still killed approximately 90% of the bacteria at 10 μg/ml. The cyclic Crp4 peptides exhibited equivalent or in some cases greater bactericidal activity than native Crp4-wt (Fig. 6). For example, cyclized Crp4–1 and Crp4–2 were more potent than native Crp4-wt against *L. monocytogenes* 10403s at 5 and 10 μg/ml concentrations. Similar results were obtained for cyclized Crp4–1 and Crp4–2 against MRSA and EPEC, respectively, at 5 mg/mL. These data demonstrate that cyclization retains the biological activity of Crp4, and for some bacterial cell targets, improves bactericidal activity.

Analysis of the antimicrobial activities in the presence of increasing NaCl concentrations showed minor differences at 160 mM NaCl, in which 10 μg/mL of native Crp4-wt killed 70% and cyclized Crp4–1 killed 80% of *L. monocytogenes* 10403s and *E. coli* ML35 (Fig. S6a and S6b). These data contrast with previous studies of cyclic rabbit NP-1, which was more active than natural NP-1 against *E. coli* in the presence of 100 mM NaCl (37). This may be due to differences in the primary structures of Crp4 versus NP-1 (Fig. 1), despite their highly similar three-dimensional folds. The antimicrobial activities of Crp4-wt and cyclic variants in the presence of 5% heat-inactivated human serum were attenuated, but 75–95% of EPEC exposed to 10 μg/mL peptide were still killed (Fig. S6C). These data suggest the cyclic Crp4 variants retain antimicrobial activity under conditions that mimic an *in vivo* environment, and therefore, have the potential to be developed as a drug lead, particularly against antibiotic resistant bacteria.

To assess the selectivity of Crp4 and cyclized Crp4 defensins, we tested the cytotoxicity of native Crp4-wt and cyclized Crp4–1 in a hemolysis assay against human red blood cells. Both peptides lacked hemolytic activity at concentrations up to 100 μg/mL, while the positive control peptide, melittin, gave approximately 75% hemolysis at the same concentration (Table 3). Additionally, native Crp4 has been found to be non-cytotoxic to the mouse macrophage cell line, RAW 264.7 (unpublished-Ouellette lab). These data demonstrate native and cyclic Crp4 are selective against bacteria.

Stability of Crp4 in human serum

Proteomics analyses of mouse colonic luminal contents have shown that intact, active α-defensins persist after secretion by Paneth cells of the small intestine (63). Cryptdin peptides have been recovered from washing of mouse jejunum and ileum (42, 47) and the distal colonic lumen (63), demonstrating their inherent resistance to proteolysis in the gastrointestinal environment conferred by the disulfide array. The stability of Crp4 was further assessed by incubation of native and cyclic peptides in 100% human serum, a location where Crp4 does not naturally occur (Fig. 7). Both the native and cyclic peptides remained intact, with no hydrolysis of the native Crp4 N- and C-termini (data not shown). In contrast, degradation of a disulfide-null mutant of native Crp4, in which the six Cys residues are mutated to Ala (Crp4–6C/A), and a S-carboxamidomethylated linear Crp4 (Crp4-R/A) (Table 1) began after just 2 min in human serum and were completely proteolyzed within 10–30 min (Fig. 7, insert). Although Crp4–6C/A maintains potent antimicrobial activity *in*

vitro, it is susceptible to degradation by matrix metalloproteinase (MMP) 7, the mouse pro-α-defensin convertase (50, 64). These stability results open the possibility of developing Crp4 as a therapeutic agent. Although native Crp4 was stable in serum for 48 h, it is possible cyclized Crp4 variants may show greater stability at longer time points or *in vivo*, when injected or fed to animals.

DISCUSSION

Defensins are innate immune peptides that play an important role in host defense of mammals. In this study, we have produced several backbone cyclized variants of a mouse α-defensin in *E. coli* cells using modified protein splicing units. The cyclized peptides were characterized by NMR, antimicrobial activities, and serum stability.

The different cyclized versions of Crp4 were produced recombinantly either *in vitro* or *in vivo*. The best expression yield was obtained for Crp4–1 when cyclized *in vitro* (≈200 μg/L). The yields for the other cyclized Crp4 variants ranged from 170 μg/L to 35 μg/L (Table 2). *In vivo* expression was by far less efficient with yields ≈2 μg/L. All of the examined cyclized Crp4 variants gave a similar yield when expressed *in vivo* independently of the precursor used. This strongly suggests that the amount of cyclized defensins that could be produced *in vivo* may be limited by the intracellular toxicity of the defensin. α-Defensins are antimicrobial compounds that can bind and disturb the membranes of bacteria and have also been shown to inhibit the biosynthesis of peptidoglycan by binding to its precursor lipid II (60, 61). It is possible that folded cyclized Crp4 may exert the same type of action when it is in the bacterial cytosol, explaining the intracellular toxicity. Our data also indicates that cyclized Crp4 variants bind strongly to the intein-CBD fusion protein, specifically to the intein region. At this time, it is unknown how the peptide is binding to the protein. It may involve electrostatic interactions with the intein since Crp4 is highly cationic and the Gyrase intein has an overall anionic charge. Interestingly, *in vivo* production of cyclized Crp4 defensins always provided the peptide on the insoluble fraction, therefore, it is possible that this occurs through binding to the insoluble intein-CBD protein. It may also be bound to insoluble bacterial membranes or cell wall precursors such as lipid II. Additional experiments to fractionate the pellet are necessary to delineate these results.

Structural characterization of the cyclized Crp4 variants by NMR revealed that they adopt structures that are very similar to that of native Crp4. This indicates that backbone cyclization did not significantly change the native fold of Crp4. The antimicrobial assays also demonstrated that backbone cyclization did not affect the biological activities of the peptide. In fact, some of the cyclized defensins showed better bactericidal activity (Fig. 6). Interestingly, native and cyclic Crp4 showed no hemolytic activity against human red blood cells demonstrating their selectivity against bacteria. Additionally, Crp4-wt and cyclic Crp4–1 defensins both demonstrated high stability to human serum, with half lives >48 h. In contrast, mutation or alkylation of the Cys residues resulted in complete degradation of the corresponding linear peptides by human serum in less than 30 min. Based on these data, it is likely the three disulfide bonds are essential components in stabilization of the peptide structures. The presence of the disulfide array has previously been shown to be a necessary component in resistance to proteolytic degradation, but does not affect antimicrobial activity (50). Altogether, these properties make cyclized Crp4 defensins promising scaffolds for drug development of novel antibiotics, although further studies may be required to evaluate their metabolic stability and bioavailability.

Novel antimicrobial agents are necessary to overcome the threat of prevalent antibiotic resistant pathogens. Based on the data reported here, this peptide can potentially be used as a stable scaffold to generate more enhanced antimicrobial drugs. Although a library of Crp4

sequences is not useful in bacterial expression systems, they have the potential to be expressed in yeast or mammalian cells providing there is no intracellular cytotoxicity. This may be useful for *in vivo* screening against intracellular pathogens, including viruses and parasites (65). Studies have shown that antimicrobial peptides can decrease the viability of intracellular *Mycobacterium tuberculosis* (66) and inhibit the proliferation of intracellular *L. monocytogenes* in macrophages (67), therefore, the expression of defensin libraries in mammalian cells is a promising method to develop and screen for more effective antimicrobials against intracellular pathogens.

Supplementary Material

Refer to Web version on PubMed Central for supplementary material.

Acknowledgments

We would like to thank Caroline Martel and Sabine Chauveau for technical assistance.We thank Dr. Annie Wong-Beringer (University of Southern California) for generously providing MRSA

clinical isolate EB378 and Dr. Gail Hecht (University of Illinois at Chicago) for EPEC strain E2348/69.

#This work was supported by National Institutes of Health Research Grant R01-GM090323 (JAC), DK044632 and AI059346 (A.J.O.), and NIH Grant 5R01GM085006-02 (AS); and by the Department of Defense Congressionally Directed Medical Research Program Grant PC09305 (JAC).

Abbreviations

CBD	chitin binding domain
CFU	colony forming unit
Crp4	cryptdin 4
DPBS	Dulbecco's phosphate-buffered saline
EDTA	ethylenediaminetetraacetic acid
EPEC	enteropathogenic *Escherichia coli*
GdmCl	guanidinium chloride
GSH	reduced glutathione
HPLC	high performance liquid chromatography
HSQC	heteronuclear single quantum coherence
IPTG	Isopropyl β-D-1-thiogalactopyranoside
NCL	native chemical ligation
NMR	nuclear magnetic resonance
MRSA	methicillin-resistant *Staphyloccocus aureus*
NOESY	Nuclear Overhauser effect spectroscopy
PIPES	1,4-piperazinediethanesulfonic acid
PMSF	phenylmethylsulfonyl fluoride
RBC	red blood cells
SFTI	sunflower trypsin inhibitor 1
TFA	trifluoroacetic acid

TOCSY	total correlation spectroscopy
TSP	trypticase soy broth
UV	ultraviolet

References

1. Unger T, Oren Z, Shai Y. The effect of cyclization of magainin 2 and melittin analogues on structure, function, and model membrane interactions: implication to their mode of action. Biochemistry. 2001; 40:6388–6397. [PubMed: 11371201]
2. Dathe M, Nikolenko H, Klose J, Bienert M. Cyclization increases the antimicrobial activity and selectivity of arginine- and tryptophan-containing hexapeptides. Biochemistry. 2004; 43:9140–9150. [PubMed: 15248771]
3. Clark RJ, Fischer H, Dempster L, Daly NL, Rosengren KJ, Nevin ST, Meunier FA, Adams DJ, Craik DJ. Engineering stable peptide toxins by means of backbone cyclization: stabilization of the alpha-conotoxin MII. Proc Natl Acad Sci U S A. 2005; 102:13767–13772. [PubMed: 16162671]
4. Adessi C, Soto C. Converting a peptide into a drug: strategies to improve stability and bioavailability. Curr Med Chem. 2002; 9:963–978. [PubMed: 11966456]
5. Camarero JA, Fushman D, Sato S, Giriat I, Cowburn D, Raleigh DP, Muir TW. Rescuing a destabilized protein fold through backbone cyclization. J Mol Biol. 2001; 308:1045–1062. [PubMed: 11352590]
6. Clark RJ, Jensen J, Nevin ST, Callaghan BP, Adams DJ, Craik DJ. The engineering of an orally active conotoxin for the treatment of neuropathic pain. Angew Chem Int Ed Engl. 2010; 49:6545–6548. [PubMed: 20533477]
7. Trabi M, Craik DJ. Circular proteins--no end in sight. Trends Biochem Sci. 2002; 27:132–138. [PubMed: 11893510]
8. Camarero JA, Muir TW. Chemoselective backbone cyclization of unprotected peptides. Chem. Comm. 1997; 1997:1369–1370.
9. Camarero JA, Cotton GJ, Adeva A, Muir TW. Chemical ligation of unprotected peptides directly from a solid support. J Pept Res. 1998; 51:303–316. [PubMed: 9560006]
10. Camarero JA, Pavel J, Muir TW. Chemical Synthesis of a Circular Protein Domain: Evidence for Folding-Assisted Cyclization. Angew. Chem. Int. Ed. 1998; 37:347–349.
11. Shao Y, Lu WY, Kent SBH. A novel method to synthesize cyclic peptides. Tetrahedron Lett. 1998; 39:3911–3914.
12. Tam JP, Lu YA. A biomimetic strategy in the synthesis and fragmentation of cyclic protein. Protein Sci. 1998; 7:1583–1592. [PubMed: 9684891]
13. Camarero JA, Mitchell AR. Synthesis of proteins by native chemical ligation using Fmoc-based chemistry. Protein Pept Lett. 2005; 12:723–728. [PubMed: 16305540]
14. Camarero JA, Muir TW. Biosynthesis of a Head-to-Tail Cyclized Protein with Improved Biological Activity. J. Am. Chem. Soc. 1999; 121:5597–5598.
15. Evans TC, Benner J, Xu M-Q. The cyclization and polymerization of bacterially expressed proteins using modified sef-splicing inteins. J. Biol. Chem. 1999; 274:18359–18381. [PubMed: 10373440]
16. Scott CP, Abel-Santos E, Wall M, Wahnon D, Benkovic SJ. Production of cyclic peptides and proteins in vivo. Proc. Natl. Acad. Sci. USA. 1999; 96:13638–13643. [PubMed: 10570125]
17. Camarero JA, Kimura RH, Woo YH, Shekhtman A, Cantor J. Biosynthesis of a fully functional cyclotide inside living bacterial cells. Chembiochem. 2007; 8:1363–1366. [PubMed: 17590879]
18. Austin J, Wang W, Puttamadappa S, Shekhtman A, Camarero JA. Biosynthesis and biological screening of a genetically encoded library based on the cyclotide MCoTI-I. Chembiochem. 2009; 10:2663–2670. [PubMed: 19780078]
19. Austin J, Kimura RH, Woo YH, Camarero JA. In vivo biosynthesis of an Ala-scan library based on the cyclic peptide SFTI-1. Amino Acids. 2009; 38:1313–1322. [PubMed: 19685144]

20. Selsted ME, Harwig SS, Ganz T, Schilling JW, Lehrer RI. Primary structures of three human neutrophil defensins. J Clin Invest. 1985; 76:1436–1439. [PubMed: 4056036]
21. Ouellette AJ, Miller SI, Henschen AH, Selsted ME. Purification and primary structure of murine cryptdin-1, a Paneth cell defensin. FEBS Lett. 1992; 304:146–148. [PubMed: 1618314]
22. Tang YQ, Yuan J, Osapay G, Osapay K, Tran D, Miller CJ, Ouellette AJ, Selsted ME. A cyclic antimicrobial peptide produced in primate leukocytes by the ligation of two truncated alpha-defensins. Science. 1999; 286:498–502. [PubMed: 10521339]
23. Tanabe H, Yuan J, Zaragoza MM, Dandekar S, Henschen-Edman A, Selsted ME, Ouellette AJ. Paneth cell alpha-defensins from rhesus macaque small intestine. Infect Immun. 2004; 72:1470–1478. [PubMed: 14977952]
24. Selsted ME, Ouellette AJ. Mammalian defensins in the antimicrobial immune response. Nat Immunol. 2005; 6:551–557. [PubMed: 15908936]
25. Niyonsaba F, Ushio H, Nakano N, Ng W, Sayama K, Hashimoto K, Nagaoka I, Okumura K, Ogawa H. Antimicrobial peptides human beta-defensins stimulate epidermal keratinocyte migration, proliferation and production of proinflammatory cytokines and chemokines. J Invest Dermatol. 2007; 127:594–604. [PubMed: 17068477]
26. Steinstraesser L, Koehler T, Jacobsen F, Daigeler A, Goertz O, Langer S, Kesting M, Steinau H, Eriksson E, Hirsch T. Host defense peptides in wound healing. Mol Med. 2008; 14:528–537. [PubMed: 18385817]
27. Yang D, Chen Q, Chertov O, Oppenheim JJ. Human neutrophil defensins selectively chemoattract naive T and immature dendritic cells. J Leukoc Biol. 2000; 68:9–14. [PubMed: 10914484]
28. Territo MC, Ganz T, Selsted ME, Lehrer R. Monocyte-chemotactic activity of defensins from human neutrophils. J Clin Invest. 1989; 84:2017–2020. [PubMed: 2592571]
29. Yang D, Liu ZH, Tewary P, Chen Q, de la Rosa G, Oppenheim JJ. Defensin participation in innate and adaptive immunity. Curr Pharm Des. 2007; 13:3131–3139. [PubMed: 17979754]
30. Rehaume LM, Hancock RE. Neutrophil-derived defensins as modulators of innate immune function. Crit Rev Immunol. 2008; 28:185–200. [PubMed: 19024344]
31. Bhattacharjya S. De novo designed lipopolysaccharide binding peptides: structure based development of antiendotoxic and antimicrobial drugs. Curr Med Chem. 17:3080–3093. [PubMed: 20629624]
32. Scott MG, Vreugdenhil AC, Buurman WA, Hancock RE, Gold MR. Cutting edge: cationic antimicrobial peptides block the binding of lipopolysaccharide (LPS) to LPS binding protein. J Immunol. 2000; 164:549–553. [PubMed: 10623792]
33. Motzkus D, Schulz-Maronde S, Heitland A, Schulz A, Forssmann WG, Jubner M, Maronde E. The novel beta-defensin DEFB123 prevents lipopolysaccharide-mediated effects in vitro and in vivo. FASEB J. 2006; 20:1701–1702. [PubMed: 16790530]
34. Droin N, Hendra JB, Ducoroy P, Solary E. Human defensins as cancer biomarkers and antitumour molecules. J Proteomics. 2009; 72:918–927. [PubMed: 19186224]
35. Rosengren KJ, Daly NL, Fornander LM, Jonsson LM, Shirafuji Y, Qu X, Vogel HJ, Ouellette AJ, Craik DJ. Structural and functional characterization of the conserved salt bridge in mammalian paneth cell alpha-defensins: solution structures of mouse CRYPTDIN-4 and (E15D)-CRYPTDIN-4. J Biol Chem. 2006; 281:28068–28078. [PubMed: 16857681]
36. Bals R, Goldman MJ, Wilson JM. Mouse beta-defensin 1 is a salt-sensitive antimicrobial peptide present in epithelia of the lung and urogenital tract. Infect Immun. 1998; 66:1225–1232. [PubMed: 9488417]
37. Yu Q, Lehrer RI, Tam JP. Engineered salt-insensitive alpha-defensins with end-to-end circularized structures. J Biol Chem. 2000; 275:3943–3949. [PubMed: 10660548]
38. Ayabe T, Satchell DP, Wilson CL, Parks WC, Selsted ME, Ouellette AJ. Secretion of microbicidal alpha-defensins by intestinal Paneth cells in response to bacteria. Nat Immunol. 2000; 1:113–118. [PubMed: 11248802]
39. Ouellette AJ, Greco RM, James M, Frederick D, Naftilan J, Fallon JT. Developmental regulation of cryptdin, a corticostatin/defensin precursor mRNA in mouse small intestinal crypt epithelium. J Cell Biol. 1989; 108:1687–1695. [PubMed: 2715173]

40. Eisenhauer PB, Harwig SS, Lehrer RI. Cryptdins: antimicrobial defensins of the murine small intestine. Infect Immun. 1992; 60:3556–3565. [PubMed: 1500163]
41. Ouellette AJ, Darmoul D, Tran D, Huttner KM, Yuan J, Selsted ME. Peptide localization and gene structure of cryptdin 4, a differentially expressed mouse paneth cell alpha-defensin. Infect Immun. 1999; 67:6643–6651. [PubMed: 10569786]
42. Ouellette AJ, Satchell DP, Hsieh MM, Hagen SJ, Selsted ME. Characterization of luminal paneth cell alpha-defensins in mouse small intestine. Attenuated antimicrobial activities of peptides with truncated amino termini. J Biol Chem. 2000; 275:33969–33973. [PubMed: 10942762]
43. Salzman NH, Hung K, Haribhai D, Chu H, Karlsson-Sjoberg J, Amir E, Teggatz P, Barman M, Hayward M, Eastwood D, Stoel M, Zhou Y, Sodergren E, Weinstock GM, Bevins CL, Williams CB, Bos NA. Enteric defensins are essential regulators of intestinal microbial ecology. Nat Immunol. 2010; 11:76–83. [PubMed: 19855381]
44. Satoh Y. Effect of live and heat-killed bacteria on the secretory activity of Paneth cells in germ-free mice. Cell Tissue Res. 1988; 251:87–93. [PubMed: 2963697]
45. Satoh Y, Ishikawa K, Oomori Y, Yamano M, Ono K. Effects of cholecystokinin and carbamylcholine on Paneth cell secretion in mice: a comparison with pancreatic acinar cells. Anat Rec. 1989; 225:124–132. [PubMed: 2817426]
46. Ouellette AJ, Hsieh MM, Nosek MT, Cano-Gauci DF, Huttner KM, Buick RN, Selsted ME. Mouse Paneth cell defensins: primary structures and antibacterial activities of numerous cryptdin isoforms. Infect Immun. 1994; 62:5040–5047. [PubMed: 7927786]
47. Selsted ME, Miller SI, Henschen AH, Ouellette AJ. Enteric defensins: antibiotic peptide components of intestinal host defense. J Cell Biol. 1992; 118:929–936. [PubMed: 1500431]
48. Sancheti H, Camarero JA. “Splicing up” drug discovery. Cell-based expression and screening of genetically-encoded libraries of backbone-cyclized polypeptides. Adv Drug Deliv Rev. 2009; 61:908–917. [PubMed: 19628015]
49. Kimura RH, Tran AT, Camarero JA. Biosynthesis of the cyclotide kalata B1 by using protein splicing. Angew. Chem. Int. Ed. 2006; 45:973–976.
50. Maemoto A, Qu X, Rosengren KJ, Tanabe H, Henschen-Edman A, Craik DJ, Ouellette AJ. Functional analysis of the alpha-defensin disulfide array in mouse cryptdin-4. J Biol Chem. 2004; 279:44188–44196. [PubMed: 15297466]
51. Figueredo S, Mastroianni JR, Tai KP, Ouellette AJ. Expression and purification of recombinant alpha-defensins and alpha-defensin precursors in Escherichia coli. Methods Mol Biol. 618:47–60. [PubMed: 20094857]
52. Puttamadappa SS, Jagadish K, Shekhtman A, Camarero JA. Backbone Dynamics of Cyclotide MCoTI-I Free and Complexed with Trypsin. Angew Chem Int Ed Engl. 2010; 49:7030–7034. [PubMed: 20715250]
53. Cavanagh J, Rance M. Suppression of cross relaxation effects in TOCSY spectra via a modified DISI-2 mixing sequence. J. Magn. Res. 1992; 96:670–678.
54. Wuthrich K. NMR of Proteins and Nucleic Acids. 1986
55. Austin J, Kimura RH, Woo YH, Camarero JA. In vivo biosynthesis of an Ala-scan library based on the cyclic peptide SFTI-1. Amino Acids. 2010; 38:1313–1322. [PubMed: 19685144]
56. Chou PY, Fasman GD. Beta-turns in proteins. J Mol Biol. 1977; 115:135–175. [PubMed: 592361]
57. Shuker SB, Hajduk PJ, Meadows RP, Fesik SW. Discovering high-affinity ligands for proteins: SAR by NMR. Science. 1996; 274:1531–1534. [PubMed: 8929414]
58. Hajduk PJ, Meadows RP, Fesik SW. Discovering high-affinity ligands for proteins. Science. 1997; 278:497–499. [PubMed: 9381145]
59. Bessette PH, Aslund F, Beckwith J, Georgiou G. Efficient folding of proteins with multiple disulfide bonds in the Escherichia coli cytoplasm. Proc Natl Acad Sci U S A. 1999; 96:13703–13708. [PubMed: 10570136]
60. de Leeuw E, Li C, Zeng P, Diepeveen-de Buin M, Lu WY, Breukink E, Lu W. Functional interaction of human neutrophil peptide-1 with the cell wall precursor lipid II. FEBS Lett. 2010; 584:1543–1548. [PubMed: 20214904]

61. Wilmes M, Cammue BP, Sahl HG, Thevissen K. Antibiotic activities of host defense peptides: more to it than lipid bilayer perturbation. Nat Prod Rep. 2011; 28:1350–1358. [PubMed: 21617811]

62. Harwig SS, Eisenhauer PB, Chen NP, Lehrer RI. Cryptdins: endogenous antibiotic peptides of small intestinal Paneth cells. Adv Exp Med Biol. 1995; 371A:251–255. [PubMed: 8525919]

63. Mastroianni JR, Ouellette AJ. Alpha-defensins in enteric innate immunity: functional Paneth cell alpha-defensins in mouse colonic lumen. J Biol Chem. 2009; 284:27848–27856. [PubMed: 19687006]

64. Ouellette AJ. Paneth cell alpha-defensins in enteric innate immunity. Cell Mol Life Sci. 68:2215–2229. [PubMed: 21560070]

65. Foureau DM, Mielcarz DW, Menard LC, Schulthess J, Werts C, Vasseur V, Ryffel B, Kasper LH, Buzoni-Gatel D. TLR9-dependent induction of intestinal alpha-defensins by Toxoplasma gondii. J Immunol. 184:7022–7029. [PubMed: 20488791]

66. Tan BH, Meinken C, Bastian M, Bruns H, Legaspi A, Ochoa MT, Krutzik SR, Bloom BR, Ganz T, Modlin RL, Stenger S. Macrophages acquire neutrophil granules for antimicrobial activity against intracellular pathogens. J Immunol. 2006; 177:1864–1871. [PubMed: 16849498]

67. Arnett E, Lehrer RI, Pratikhya P, Lu W, Seveau S. Defensins enable macrophages to inhibit the intracellular proliferation of Listeria monocytogenes. Cell Microbiol. 13:635–651. [PubMed: 21143570]

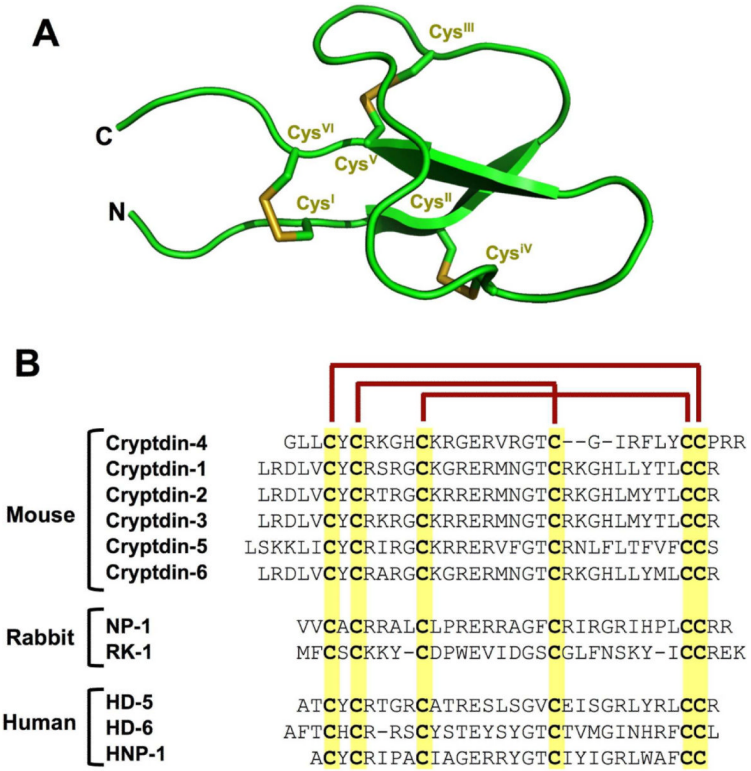

Figure 1.

(**A**) Tertiary structure of Crp4 (PDB code: 1TV0) (35). (**B**) Primary structures of representative α-defensins from mouse, rabbit, and human. The six conserved cysteines are highlighted and the canonical 1–6, 2–4, 3–5 disulfide connectivities are shown at the top of the sequences.

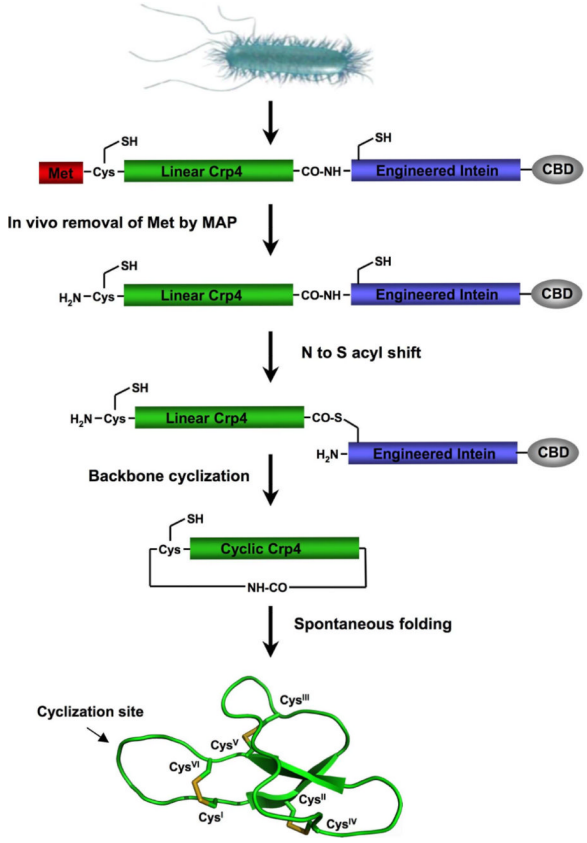

Figure 2.

Biosynthesis of backbone cyclized Crp4 variants using a modified intein in combination with native chemical ligation. CBD stands for chitin binding domain.

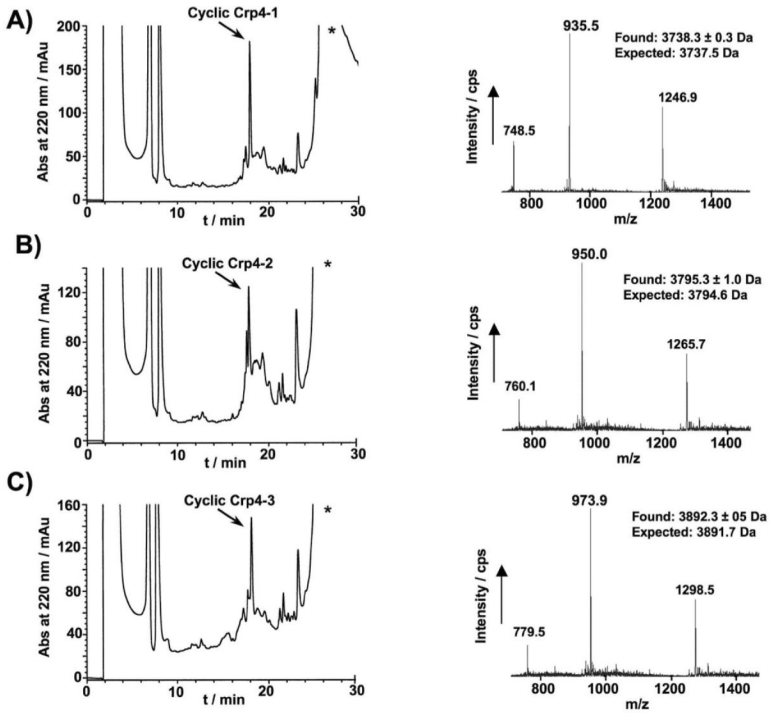

Figure 3.

In vitro GSH-induced cyclization of precursors Crp4–1 (**A**), Crp4–2 (**B**), and Crp4–3 (**C**). On the left are the RP-HPLC chromatograms of the crude reaction and on the right is the ES-MS of the corresponding cyclic folded product indicated with an arrow. The large peak labeled with an asterisk is the intein-CBD protein. Experimental and theoretical molecular weights are shown with MS spectra.

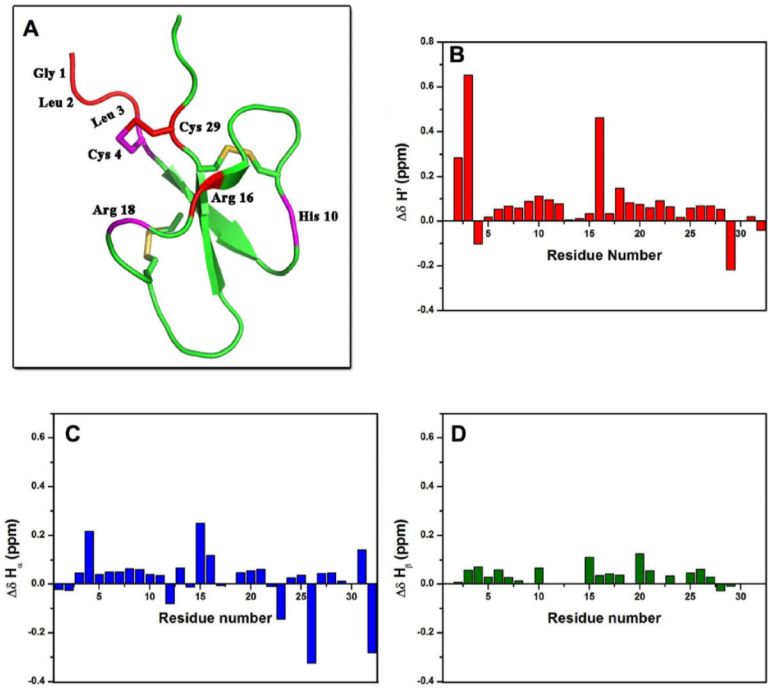

Figure 4.

Chemical shifts differences of the backbone, H' and H^a. and side chain, H^b. protons between cyclic Crp4–1 and native Crp4-wt. (**A**) The ribbon diagram of native Crp4-wt shows the residues that exhibit a significant change in the chemical shift of the backbone amide after cyclization. Residues with a change in chemical shift larger than 0.2 pmm or between 0.1 and 0.2 ppm are in red and magenta, respectively. Changes in the H' (**B**), H^a (**C**) and H^b (**D**) chemical shifts between native Crp-wt and cyclic Crp4–1 defensins reflect minimal structural perturbations due to cyclization.

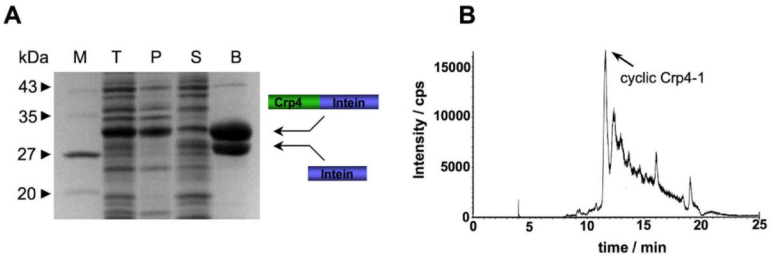

Figure 5.

In vivo expression of cyclic Crp4–1 defensin in Origami2(DE3) cells. (**A**) SDS-PAGE analysis of the expression of Crp4-intein precursor Crp4–1. M: molecular weight protein markers, T: total cell lysate, P: insoluble cell lysate, S: soluble cell lysate and B: affinity chromatography purified Crp4-intein precursor. (**B**) Mass spectrum of the insoluble cell lysate following HPLC separation (see Experimental Section).

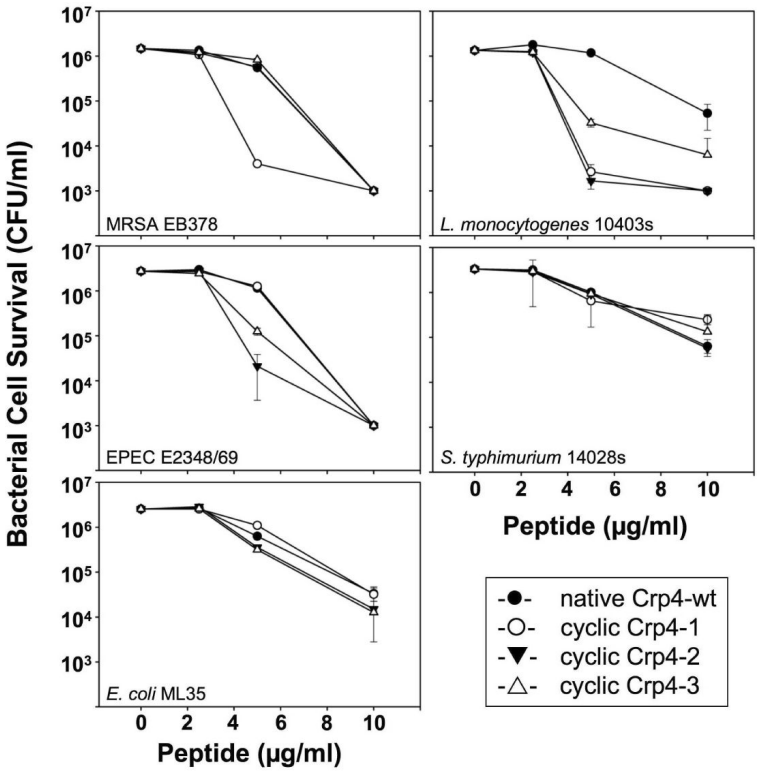

Figure 6.

Bactericidal activities of Crp4-wt and cyclic Crp4 variants. Exponentially growing MRSA, *L. monocytogenes* 10403s, EPEC E2348/69, *S. typhimurium* 14028s, and *E. coli* ML35 were exposed to peptides at 37°C in 50 μL of PIPES-TSB buffer for 1 h (see Materials and Methods). Following peptide exposure, the bacteria were plated on TSB-agar plates and incubated overnight at 37°C. Surviving bacteria were counted as CFU at each peptide concentration, and count values below 1×10^3 CFU/mL signify that no colonies were detected.

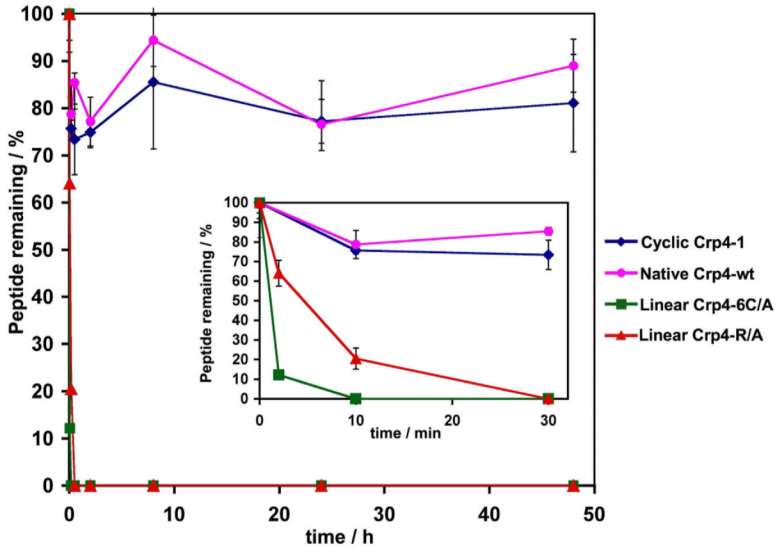

Figure 7.

Stability of Crp4 and variants in human serum. Peptides at 100 μg/mL were incubated with heat-inactivated serum at 37 °C and analyzed by C4 RP-HPLC. Linear Crp4–6C/A is a native Crp4-wt variant in which the six Cys are mutated to Ala. Linear Crp4-R/A corresponds to a linear Crp4–1 construct in which the six Cys are alkylated with iodoacetamide.

Intein precursor	Sequence
Crp4-1	CYCRKGHCKRGERVRGTCGIRFLYCCPRRGLL-intein
Crp4-2	CYCRKGHCKRGERVRGTCGIRFLYCCPRRGGLL-intein
Crp4-3	CYCRKGHCKRGERVRGTCGIRFLYCCPRRGPGLL-intein
Crp4-4	CRKGHCKRGERVRGTCGIRFLYCCPRRGLLCY-intein
Crp4-5	CCPRRGLLCYCRKGHCKRGERVRGTCGIRFLY-intein

Scheme 1.

Sequences of the different Crp4-intein precursors used in this study. The first three residues located at the N-terminus of Crp4-wt are underlined in blue for reference. The residues added to the ligation site to facilitate cyclization are shown in green.

Table 1

Amino acid sequences of the Crp4 peptides used in this study.

Peptide	Sequence
Crp4-wt	GLLCYCRKGHCKRGERVRGTCGIRFLYCCPRR
Crp4-6C/A	GLLAYARKGHAKRGERVRGTAGIRFLYAAPRR[2]
Crp4-1	cyclo[CYCRKGHCKRGERVRGTCGIRFLYCCPRRGLL]
Crp4-2	cyclo[CYCRKGHCKRGERVRGTCGIRFLYCCPRRGGLL][3]
Crp4-3	cyclo[CYCRKGHCKRGERVRGTCGIRFLYCCPRRGPGLL][3]
Crp4-R/A	CYCRKGHCKRGERVRGTCGIRFLYCCPRRGLL[4]

[1] The first three amino acids of the Crp4 natural N-terminus are shown in blue for reference.

[2] Ala residues replacing original Cys residues are marked in magenta

[3] The linkers added to assist in cyclization are shown in green.

[4] Cys residues reduced and alkylated are underlined.

Table 2

Expression yields and cleavage percentages of Crp4-intein precursors in BL21(DE3) cells, and yields of cyclic/folded Crp4 variants after *in vitro* cleavage of the intein.

Precursor	Yield (mg/L)		% of soluble intein cleaved		Yield[3], μg/L (%)
	S[1]	p[2]	in vivo	in vitro	cyclic/folded
Crp4-1	5.5	142.1	23.9	84.2	200 (50%)[4]
Crp4-2	9.8	24.7	22.9	73.4	120 (20%)[4]
Crp4-3	10.5	94.3	20.7	70.4	174 (27%)[4]
Crp4-4	9.0	0	29.1	67.7	43 (10%)[4]
Crp4-5	13.9	0	7.5	45.6	35 (5%)[4]

[1] Soluble cell lysate fraction.

[2] Insoluble cell lysate fraction

[3] Obtained after *in vitro* cleavage with GSH (see Experimental Procedures).

[4] Cyclization/folding yield is based on the amount of precursor cleaved during the GSH-induced in vitro cleavage.

Table 3

Hemolytic activities of native and cyclized Crp4 defensins. The peptide melittin was used as a control.

Peptide	Concentration (μg/mL)					
	0	**1**	**12.5**	**25**	**50**	**100**
Crp4-wt	4.2%	n/d[1]	4.1%	3.4%	3.0%	3.1%
Crp4-1	4.2%	n/d[1]	5.4%	5.8%	5.9%	4.9%
Melittin	4.2%	3.6%	n/d[1]	n/d[1]	n/d[1]	74.6%

[1] n/d: not determined